

Inspection and Evaluation of Wood Components of Ancient Buildings in the South-Three Courts of the Forbidden City

Yongjie Tan, Xiaojun Yang,* Xinchun Bai, Haoran Dong, Jiamin Liu and Lu Zhang

Ancient architectural wood components were evaluated in terms of mechanical properties, material color expression, ultrasonic shape, chemical components, and deformation of shape and position by comparing them with new red pine materials. The results showed that the deterioration of the surface material properties of wood components was very serious, mainly caused by weathering. The attenuation degree of the inner layer of the wood component was relatively low, and the color change of the wood was obvious, which was mainly caused by fungi. Ultrasonic nondestructive testing technology was used to detect the internal damage of ancient wood components. According to the test results, it was speculated that the root defects of pillar components were serious. Three components of wood after long-term weathering changed significantly, and lignin had been seriously damaged. This damage was reflected in the degradation of the number of aromatic groups and the changes in the nature of the group. The main wood beams in the main halls of the three yards were bent at 0 mm offset scale and unit offsets of the pillars of the four courtyards were within the safe range.

DOI: 10.15376/biores.17.1.962-974

Keywords: Forbidden City; Wood components; Wood properties; Form and position

Contact information: College of Material Science and Engineering, Nanjing Forestry University, Nanjing 210037, China; *Corresponding author: yxj5460@163.com

INTRODUCTION

Chinese culture includes wood-frame architecture. Many ancient wood structures have been damaged, and even the Forbidden City has not been spared (Geng 2018). The Forbidden City in Beijing is one of the largest and best-preserved wood structures in the world and is listed as a World Heritage Site. Some of the Forbidden City buildings have been damaged by wind, sun, rain, human damage, and biological damage, and the components have been damaged by decay, cracking, and weathering (Dai and Liang 1987; Yin *et al.* 1987; Spriggs *et al.* 1989). This damage affects the aesthetics and performance of the building and threatens the safety of tourists; thus, it must be repaired (Mosoarca and Gioncu 2013). Precious cultural heritage is a corroboration of the study of history, and it is necessary to protect, inherit, and preserve its original appearance (Shi *et al.* 2009). The country attaches great importance to the restoration and protection of the Forbidden City. As early as 2002, the “Forbidden City overhaul” plan was launched (Qin *et al.* 2018). Shi *et al.* (2009) investigated the Hall of Supreme Harmony and discovered its existing symptoms. According to GB 50005 (2017) standard for design of timber structures, the strength of the elements was verified by arithmetic analysis to meet the requirements, and the parts that needed strengthening were reinforced (Chang *et al.* 2019). Qin *et al.* (2018)

selected the wood structure of the well pavilion in the Forbidden City of Beijing, which has the characteristics of ancient architecture of the Ming and Qing dynasties and studied its dynamic characteristics. The self-vibration frequency of the wood structure was relatively low, and the residual damage of materials, components, and nodes reduced the structural stiffness and self-vibration frequency. Under the action of ground vibration, the horizontal reaction force of the pillar foot of the residual structure was smaller than that of the intact model, while its acceleration and displacement response were significantly larger than that of the intact structure (Qiao *et al.* 2016). Often, the restoration and protection of ancient buildings has resorted to experience and judgment based on surface observations to carry out selective repairs, and there is a lack of necessary testing for the materials of building components (Fu *et al.* 2021). Repairs are difficult or insufficient, which is not conducive to protecting the original appearance of the building and its components (Parisi and Piazza 2007; Lu 2017). Before starting the restoration project of ancient buildings, it is an important measure to scientifically protect the ancient buildings and cultural relics after testing and analysis of the buildings and their components (Wang *et al.* 2019; Zhang *et al.* 2021).

South-Three Courts is the palace building of the Forbidden City in Beijing. As shown in Fig. 1, the Emperor Jiaqing once lived (Shan 1988) there. South-Three Courts shares a palace gate, with 3 rooms wide and 1 room deep. It has a green glazed tiled mountain top. The door opens in the middle, and there is a ramp with a sawtooth slope made of brick or stone inside and outside. South-Three Courts is located in the eastern part of the Forbidden City. According to the five elements of yin and yang, the east relates to wood, green, the main growth, and so the roof is covered with green glazed tiles and arranged for the imperial son to live here. The roofs of South-Three Courts are single eaves hard hill roof or hipped roof; the form of the emperor's temple used a slightly inferior grade. The architectural complex of South-Three Courts includes the first courtyard, second courtyard, third courtyard, and fourth courtyards, where the first courtyard, second courtyard, and third courtyard include the main hall, East Hall, East Hall South ear room, East Hall North ear room, West Hall, West Hall South ear room, West Hall North ear room, where four halls include the West Hall and rear hooded rooms, and other buildings (Shan 2016). In this paper, the beam and pillar elements replaced during the repair of South-Three Courts of the Forbidden City were studied, compared with new red pine material, and their material characteristics were studied in terms of mechanical properties, material color performance, ultrasonic shape, chemical components, and deformation of form, to make a preliminary determination of the material and facilitate measures for the repair and protection of ancient wooden buildings in China.

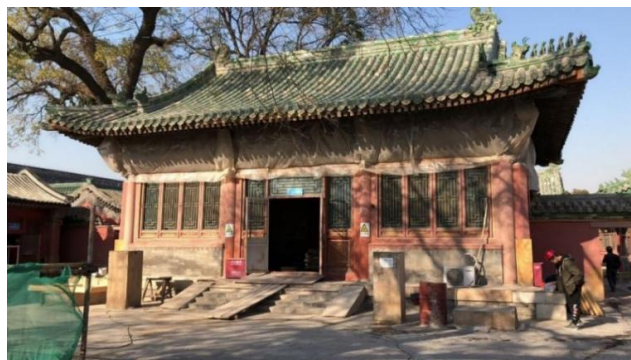


Fig. 1. The main hall of the first courtyard of South-Three Courts

EXPERIMENTAL

Materials

The test wood is the old material dismantled during the maintenance of South-Three Courts of the Forbidden City. The main species is *Pinus koraiensis*, taken from the beams, pillars, and Fang, which according to historical records have served about 134 years, and all of which have varying degrees of decay. The moisture content was about 14%. The comparison material was new red pine (*Pinus koraiensis*) from the northeast of China, with some live joints and cracks and straight grain.

The experimental instruments and equipment were a CR-10 portable colorimeter (Konica Minolta Group, Tokyo, Japan), a UTM4304 universal mechanical testing machine (Suns Technology, Shenzhen, China), a BJNM-1 intelligent non-metallic ultrasonic detector (Beijing Institute of Optoelectronics Technology, Beijing, China), a Fourier transform infrared spectrometer (FTIR) (PerkinElmer, Massachusetts, USA), a laser five-line meter (Hi Fidelity Technology, Beijing, China), and a laser skew tester (NADO Intelligent Technology, Yantai, China)

Experimental Design

The test detected the old wood components of the Forbidden City and evaluated their material properties. At the same time, it analyzed how its performance compared with the new red pine produced in the northeast of China, and it studied the degree of material color difference between the surface and the inside of the component, so as to establish the corresponding relationship between the color of the component and the material performance. In addition, ultrasonic nondestructive testing, FTIR, and shape testing tests were performed on the wood components.

The test was divided into two parts. The first part was the field collection, which was planned to conduct color testing, ultrasonic flaw detection, and form testing on some of the beams, pillars, and Fang at South-Three Courts, and to collect some of the components replaced during maintenance for further testing in the laboratory.

The second part was carried out in the laboratory. The old wood components were divided into 3 groups, L, Z, and F, according to the part from which they were taken, with 3 groups of L components, 4 groups of Z components, and 2 groups of F components. Six control groups for flexural and modulus of elasticity tests of new wood and three control groups for hardness tests were also planned.

The test procedure was as follows: all old wood components were subjected to material color determination and ultrasonic nondestructive testing, followed by tests of flexural strength and modulus of elasticity for L1, Z1, and F1, hardness tests for L2, Z2, and F2, and finally, infrared spectra were measured for L2. Each group of experiments was conducted with new red pine as the control group of the specimens.

Methods

The mechanical test method utilized the bending resistance test using the determination method of the three-point bending test, and the hardness test was conducted with reference to GB/T 1941-2009 (2009). The bending resistance specimen sampling schematic diagram is shown in Fig. 2. The thickness of all samples is 8 mm, and the length is 225 mm. The width of the beam L specimen and the column Z specimen is 40 mm. The width of the Fang F specimen and the red pine material X specimen is 50 mm.

Inner layer Outer layer

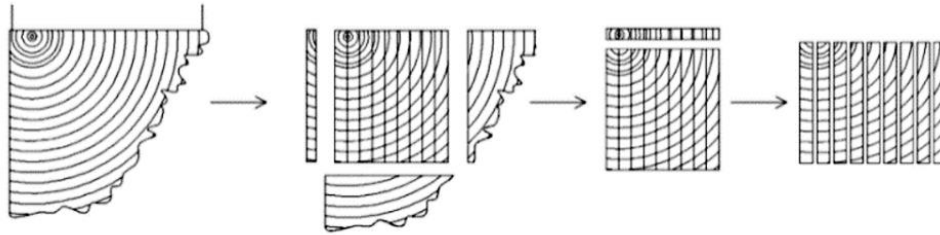


Fig. 2. Sampling schematic diagram of L1, Z1, and F1

The color difference test method was utilized. The material color was collected from the specimen, each test point was measured twice, the innermost measured point was taken as the standard point, the average value of L^* , a^* , and b^* was taken as the final color index of the position, and the color difference ΔE was calculated according to formula (1).

$$\Delta E^* = \sqrt{(L_1^* - L_2^*)^2 + (a_1^* - a_2^*)^2 + (b_1^* - b_2^*)^2} \quad (1)$$

The ultrasonic flaw detection test method was utilized in the healthy new red pine to create artificial defects, with a double probe penetration method for healthy material and defective material to test, with each test before the two probes applying an appropriate amount of petroleum jelly for coupling agent. The schematic diagram of the artificial defects is shown in Fig. 3.

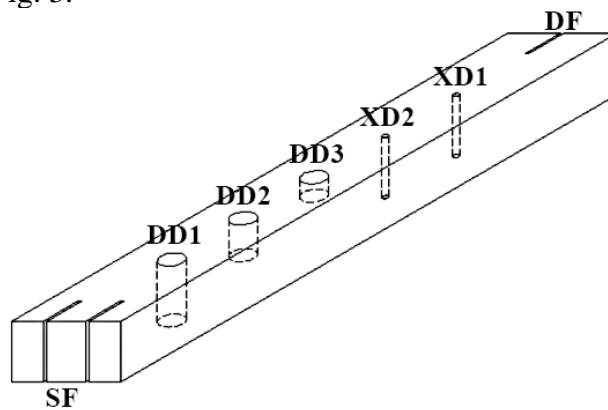


Fig. 3. Schematic diagram of artificial defects

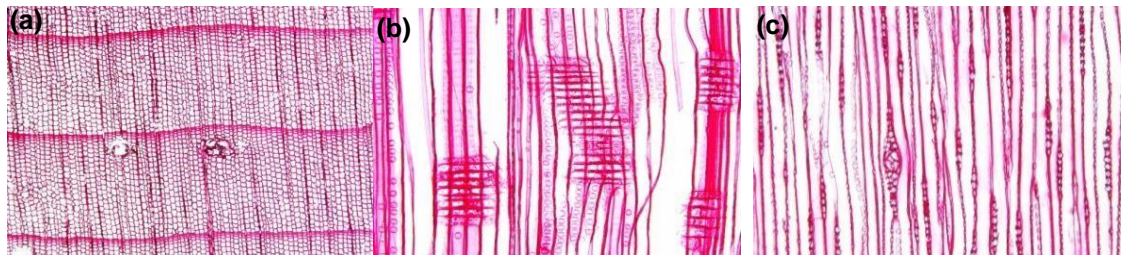
The FTIR test method was utilized. The appropriate amount of wood chips was sawn on both sides of the specimen, fully ground in an agate mortar, and pressed. Then the FTIR infrared scanning analysis was carried out using an FTIR spectrometer in the wavelength range of 400 to 4000 cm^{-1} according to the order from inner layer to outer layer.

The deformation test method was utilized. The deflection tester and laser distance meter were used in combination with traditional test methods to test the deformation of 95 pillars and 12 wood beams of the large wood structure of each building unit in South-Three Courts.

RESULTS AND DISCUSSION

Analysis of Tree Species Identification of Wood Components

The species identification was conducted on 67 key wood components taken from the eaves of the west side hall of the third courtyard, the wood pillars placed in the second courtyard, and the wood blocks on the ground of the north penthouse of the west side hall of the first courtyard. The identification procedures included slicing, soaking, microscopic observation, and photographing. A typical microscopic test photograph is shown in Fig. 4. Based on the observed species characteristics, and after consulting literature (Cheng *et al.* 1992; Jiang and Peng 2001), the species identified were mainly *Pinus koraiensis* and partly *Pinus sylvestris*.



(a) Cross section *Pinus koraiensis* (b) Vertical section *Pinus koraiensis* (c) Tangential section *Pinus koraiensis*



(d) Cross section *Pinus sylvestris* (e) Vertical section *Pinus sylvestris* (f) Tangential section *Pinus sylvestris*

Fig. 4. Microscopic photographs of specimens

The main load-bearing components of the main hall, the auxiliary hall, and the penthouse included large wood components such as pillars, three beams, and five beams. The main wood species for these wood components were *Pinus koraiensis*, *Pinus sylvestris*, and *Abies fabri*. The main species for secondary load-bearing components such as Sui beam, ceiling beam, and short pillar were *Pinus koraiensis*, *Cunninghamia lanceolata*, *Picea asperata*, and *Abies fabri*. The main selection tree species for purlins and beams were *Pinus koraiensis* and *Larix gmelinii*. In addition, cypress, hard pine, and other species were also scattered among the selected species. The proportion of each species in the overall sampling number of components is shown in Fig. 5.

As shown in Fig. 5, the main load-bearing wood components of the South-Three Courts' halls and ears were selected mainly from the northern species of hard pine for density and mechanical strength, and the other wood components mainly used were low density, light weight softwood pine. The woods used for the wall panels, ceilings, and window frame fans of the main hall, auxiliary hall, and penthouse were mainly *Pinus sylvestris*, *Cupressus funebris*, *Larix gmelinii*, *Cunninghamia lanceolata*, *etc.* The wood used by them was rather miscellaneous, which may be related to the renovation projects in different years. According to the different load-bearing nature and position of the

components, the species configuration of the South-Three Courts not only considered the strength requirements of the main building structural materials, but also considered as much as possible to reduce the load of other wood components on the main components.

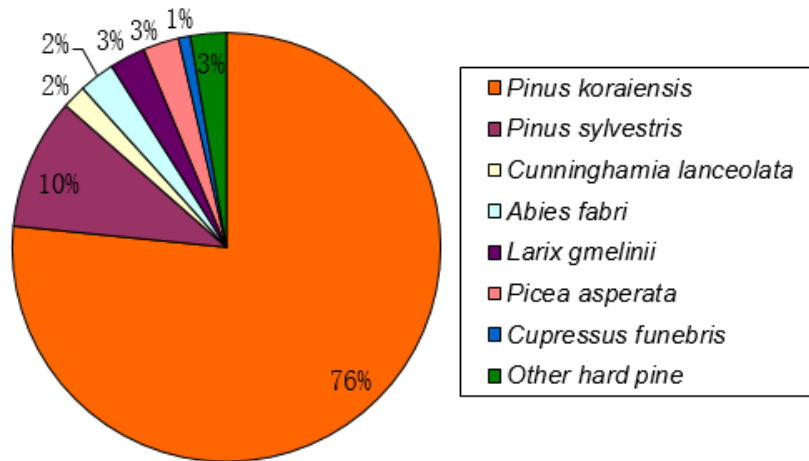


Fig. 5. The proportion of each species to the overall number of components sampled

Analysis of the Material Mechanical Decay of Wood Components and Correlation with the Color of Wood

Figure 6 shows the change curves of bending performance at different parts of the same component. The position of the sample is numbered from the innermost layer. The smaller label is close to the innermost layer, and the larger label is close to the surface. Fig. 7 shows the variation curves of hardness of chord surface.

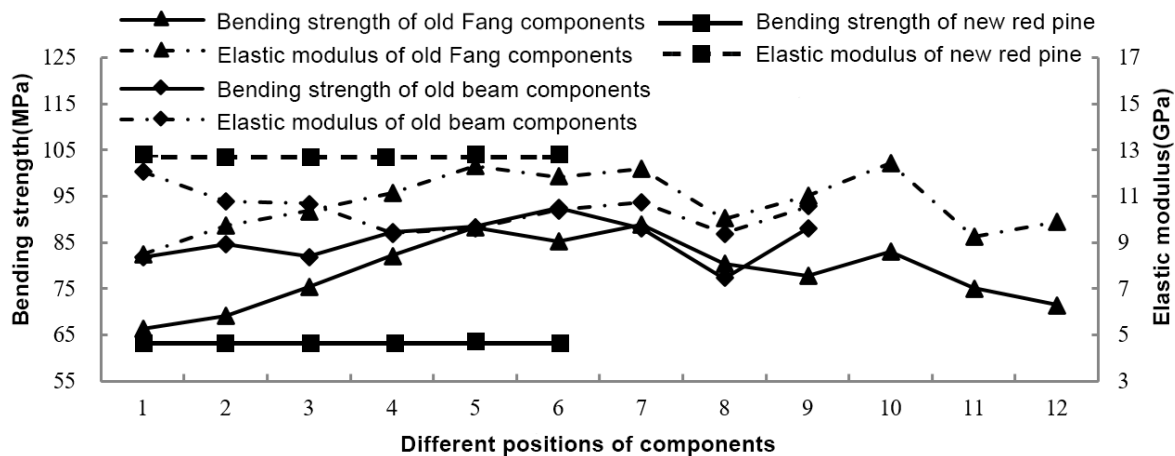


Fig. 6. Bending property of different positions of component

It can be seen from Figs. 6 and 7 that the bending strength of beam components and beam components and the elastic modulus of beam members almost all show the same rule from the innermost layer to the outermost layer. The rule is that the innermost and outermost layers are smaller and the middle layer is larger. The reason for the lower flexural strength and modulus of the outermost layer of wood is that the wood components have been severely weathered after long-term service, the surface is dark black, and the wood degradation is more serious. The innermost layer is lower because it is close to the medulla,

and its material is lower than that of sapwood. The higher innermost elastic modulus of beam members may be due to the variability of the wood material. The elastic modulus of the surface layer of the old material has a larger attenuation range than that of the new material, and the beam components and Fang components are reduced by 20.4% and 28.4% respectively. The flexural strength has been improved compared with the new red pine material, and the flexural strengths of beams and Fang have increased by 20.4% and 3.3% respectively. The old wood components use mature red pine wood with a long growth cycle, while the new material uses thinned wood. There are certain differences in the wood materials of different growth years. The old wood components experience long-term service, and the surface layer is prone to be more serious. Due to the weathering, the inner wood is susceptible to fungal erosion (Liu *et al.* 2009; Zhao *et al.* 2021), and it is mostly manifested as an old color. The average hardness of beams and beams is close to that of the new red pine material, and the hardness cannot directly reflect the difference in the properties of the new and old materials. The hardness of the inner and outer layers of beam members is obviously different, and the hardness of the innermost layer of wood is obviously higher than that of the surface layer. It shows that the material decay caused by the combined action of weathering and fungi gradually weakens from the surface to the inside. The difference in hardness between the inner and outer layers of the beam is small, indicating that the materials of the inner and outer layers of the beam are similar, and the sampled specimens have a lower degree of deterioration.

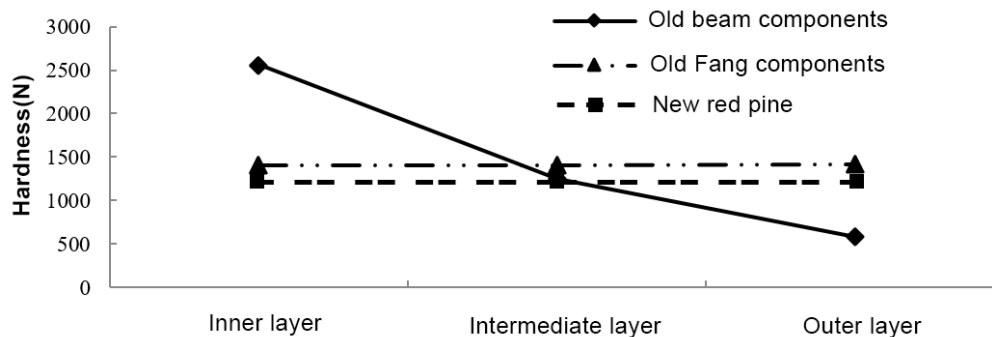


Fig. 7. Hardness of different layers of components

In the correlation test between color and mechanical properties, all three groups of old wood components showed the same pattern. The average values of the mechanical properties and color difference of each layer for the old material of the pillar components, for example, are shown in Table 1.

It can be seen from Table 1 that the color difference between the inner and outer layers of the old material of the wooden column member is obvious. The chromatic aberration of the inner layer of the wooden column is low, and the chromatic aberration of the outer layer is higher. The mechanical properties of wood in areas with lower chromatic aberration are obviously better than wood in areas with larger chromatic aberration. The chromatic aberration can reflect the difference between the inner and outer layers of the old material of the wooden pillar. In addition, on-site testing found that when the color difference of the surface of the wooden column is more than 9, the wood in this area is mostly bad and it usually needs to be replaced or taken necessary measures to repair and strengthen.

Table 1. Mechanical Properties and Color Difference of Each Layer of Aged Pillar Component

Different Positions of Components	Elastic Modulus E (GPa)	Bending Strength σ (MPa)	Hardness H (N)	Chromatic Aberration ΔE
Inner layer	11.79	99.23	2560	6.15
Intermediate layer	9.88	93.34	2670	6.95
Outer layer	9.39	90.77	2360	8.98

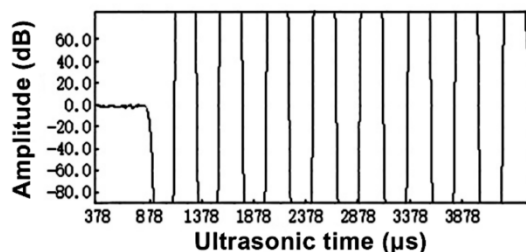
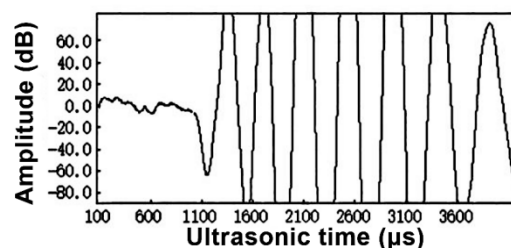
Wood Pillar Ultrasonic Flaw Detection Analysis

To study the internal defects of the old wood components, healthy and new red pine with artificial defects as the object of study for the ultrasonic flaw detection comparison test were used to obtain the wave speed, propagation time, and waveform changes in the law before the analysis of the old wood components. The ultrasonic propagation time and velocity of new red pine with different artificial defects are shown in Table 2.

Table 2. Influence of Artificial Defects on Propagation Time and Wave Velocity

Set Code	Dimensions (cm)	T (μ s)	V (km/s)
XD1	0.6 \times 5.3	49.95	1.80
DD1	2.5 \times 5.3	52.05	1.73
DD2	2.5 \times 3.2	51.45	1.75
DD3	2.5 \times 1.6	50.35	1.79
DF	6.9	61.95	1.45
SF	7.0	63.75	1.41

When the hole depth was the same and the hole size was increased to 2.5, the ultrasonic wave propagation time increased by 4.2% and the propagation speed decreased by 3.9%. When the hole size was the same and the hole depth increased to 5.3, the ultrasonic wave propagation time increased by 3.4% and the propagation speed decreased by 3.4%. Compared with one crack, the ultrasonic wave propagation time increased by 2.9% and the propagation speed decreased by 2.8% when there were two cracks. This showed that the propagation speed of ultrasonic waves was negatively correlated with the number of cracks, aperture size, and depth, and the propagation time was positively correlated with the number of cracks, aperture size, and depth. The typical ultrasonic waveforms of healthy red pine new and red pine new with artificial defects (DD1) are shown in Figs. 8 and 9. When there were large and deep holes and cracks in the interior, the amplitude of the first wave of the ultrasonic became smaller, and the waveform law changed. For the through holes and through cracks, the ultrasonic waveform was similar.

**Fig. 8.** Ultrasonic waveform of healthy wood**Fig. 9.** Ultrasonic waveform of DD1

Based on this rule, the waveform of the pillar root collected in the field (Fig. 10) was analyzed, and it was found that the waveform was similar to that of the defective new red pine. It was speculated that the root of the old material of the pillar component was seriously rotten. The old wood components were also tested. It was speculated that there were serious defects in Z1, Z2, Z3, Z4, and F1 components. Taking component Z1 as an example, the typical waveform is shown in Fig. 11.

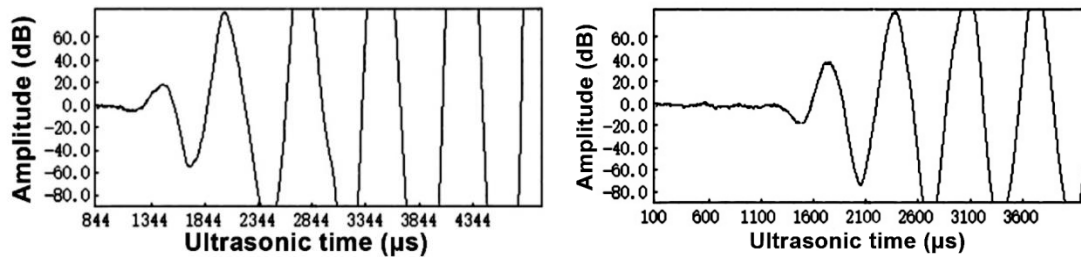


Fig. 10. Ultrasonic waveform of the bottom of pillar Fig. 11. Ultrasonic waveform of Z1

Analysis of Infrared Spectral Characteristics of Wood Component Materials

The FTIR spectra of the old material and the new material of Korean pine for beam components were analyzed, and the results are shown in Fig. 12. Sample 1 to sample 6 were taken from different parts of the beam, and transition from the out layer to the inner layer, and the order of 1 to 6 was the transition from the surface layer to the inner layer. Sample 1 was the outermost layer, and sample 6 was the innermost layer. Sample X was taken from the new pine wood.

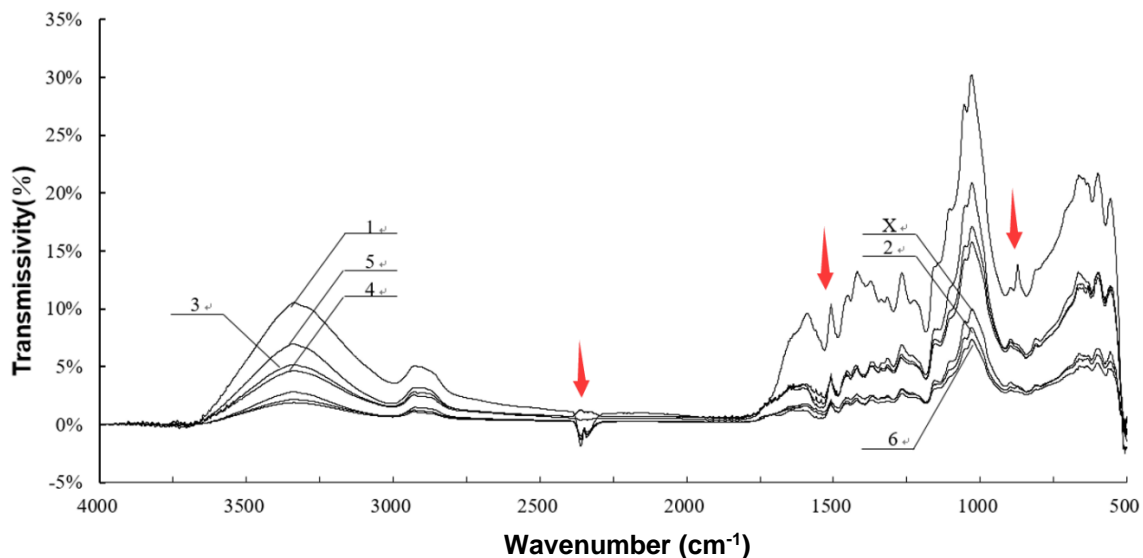


Fig. 12. Infrared spectrogram of old components and new red pine

It can be seen from Fig. 12 that after long-term weathering, the lignin, cellulose, and hemicellulose on the surface of the wood had undergone significant changes. At the same time, the difference in the inner layer of wood is not significant. The spectrum shape of sample 1 at 1585 to 1220 cm^{-1} and 940 to 835 cm^{-1} was different from other samples, indicating that the lignin and cellulose of sample 1 may have been severely damaged. The

aromatic skeleton vibration peak near 1510 cm^{-1} indicates that the lignin of sample 1 has been severely damaged. This damage is not only reflected in the degradation of the number of groups, but may also be reflected in the changes in the nature of the groups. The change is irreversible. The absorption peak at 1425 cm^{-1} comes from CH_2 shear vibration, indicating that the cellulose of sample 1 is also seriously damaged. Hemicellulose was also degraded, which is mainly reflected in the stretching vibration of the $\text{C}=\text{O}$ group near 1730 cm^{-1} . It is worth noting that not only the hemicellulose contains $-\text{OH}$ groups, but the moisture in the wood also contains $-\text{OH}$ groups. Therefore, it is difficult to judge the change of hemicellulose based only on the degradation of this group. And FTIR infrared spectroscopy can only qualitatively analyze whether there is or whether there is serious degradation. The degree of degradation cannot be quantitatively analyzed. In addition, in the range of 2380 to 2310 cm^{-1} , the waveforms of samples X, 1, 2, and 6 have been significantly collapsed. At the same time, the waveforms of samples 3, 4, and 5 have not been collapsed in the figure. However, the attribution of the absorption band in this region is still unclear.

Test and Analysis of Shape and Position Deformation of Wood Components

The shape and position deformation of 95 pillars and 12 wood beams of the large wood structure of each building unit in the South-Three Courts were tested. The unit offset curve results of the pillars of each hall in the four courtyards are shown in Fig. 13.

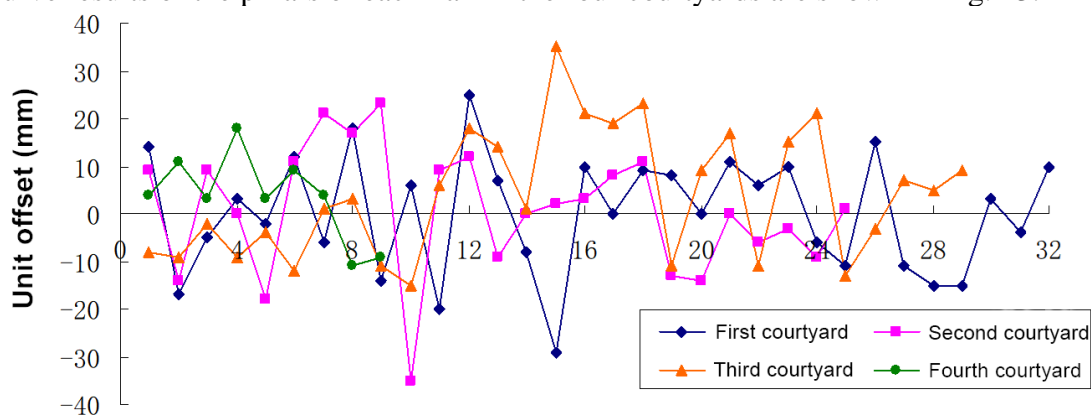


Fig. 13. Unit offset curves of the pillars of the four courtyards

As can be seen in Fig. 13, the four courtyards of each temple block pillar unit offset degree were within $\pm 40\text{ mm}$, which accounted for about 92% of the pillar unit offset degree within $\pm 20\text{ mm}$. The unit deviation degree was the deviation displacement from the hanging vertical line within a 1.2 m length range. It reflects that due to factors such as static roof load, environmental temperature and humidity, and wood activity degradation, the pillar was prone to a certain degree of shape and position shift during long-term service. When the building was in the range of $\pm 100\text{ mm}$, the offset of the pillar had little effect on the structure and structural components and could be ignored. The height of the South-Three Courts was smaller for the one-story building, and the building pillars were all large wood components, the size was much larger than the calculated value of the structural components, and the surplus was too large.

The results of the verticality curve on the surface of the pillars of the four courtyards are shown in Fig. 14.

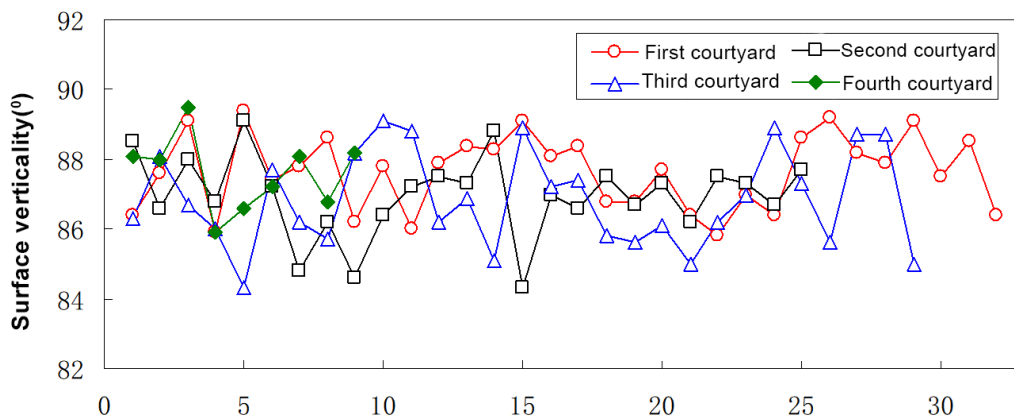


Fig. 14. Surface verticality curve of the pillars of the four courtyards

As can be seen in Fig. 14, the surface verticality of the pillars of each entry hall block was in the range of 84° to 90° , among which the pillars with surface verticality in the range of 84° to 86° account for 13.68% of the total, and the pillars in the range of 84° to 85° account for 4.21% of the total. The surface verticality can reflect the local deformation of the pillar. Theoretically, the surface of each pillar should be close to 90° , but the pillars are often affected by structural construction, service cycle, environmental erosion, and other factors, which easily lead to the phenomenon of large deviation of verticality on the pillar surface. The verticality deviation of the front eaves pillar of the west matching hall of the Second courtyard was relatively large, but it was within the safe range. It can be seen that the local deformation of the pillars of each temple was small, and they were in a safe range, and the pillars were relatively stable during service.

By using the laser indication offset method, the bending offset scale of the main wood beams of the first, second, and third courtyards of the South-Three Courts was 0 mm, including longitudinal beams, partition beams, and cross beams. The longitudinal and transverse long and short beams did not appear to have bending or deflection, indicating that the structure of each temple in the South-Three Courts as a whole or locally did not appear laterally tilted. The mechanical redundancy of large timber components was large, the foundation does not appear to have settlement, the protection measures for hundreds of years were appropriate, the beam did not appear to have deflection, and the structural safety can continue to serve in the structure.

CONCLUSIONS

1. A total of eight species or genera of wood were used in the South-Three Courts. The main load-bearing wood components in the main hall, auxiliary hall, and ear room of the South-Three Courts are mainly *Pinus koraiensis*, *Pinus sylvestris*, and *Larix gmelinii* with high density and mechanical strength of the northern tree species. Among them, the *Pinus koraiensis* species accounted for the highest proportion, accounting for 76% of the total component sampling number and *Pinus sylvestris* species accounted for 9% of the total component sampling number.
2. The deterioration of the surface material properties of wood components is more serious, mainly caused by weathering. The attenuation degree of the inner layer of the

wood component is relatively low, and the color change of the wood is obvious, which is mainly caused by fungi. Compared with the new red pine material, the elastic modulus of the old red pine material has a larger attenuation range, and the average bending strength and hardness have been improved.

3. Ultrasonic nondestructive testing technology can be used to detect the internal damage of ancient wood components and can determine whether there are serious defects such as decay and cracking. According to the results of ultrasonic nondestructive testing, it is speculated that the internal defects of pillar components were serious, followed by the Fang components, and the damage of the beam components was light.
4. After long-term weathering, the lignin and cellulose on the surface of the wood had been severely damaged. This damage was not only reflected in the degradation of the number of groups but may also be reflected in the changes in the nature of the groups, and this change was irreversible. The main degradation in the FTIR spectra was the aromatic skeleton vibration of lignin. The thickness of the lignin-depleted layer of wood at the surface is estimated to be within 3 to 4 mm. From the FTIR spectroscopy, only qualitative analysis can be performed on whether degradation has occurred, and the degree of degradation cannot be quantitatively analyzed.
5. The South-Three Courts are one-story buildings with small height and large wood pillars, which are much larger than the calculated values of structural components. In addition, the protection measures for hundreds of years are appropriate, and the beam does not appear to have deflection. The structural safety can continue to serve in the structure.

ACKNOWLEDGMENTS

This work was supported by the National Natural Science Foundation of China (Grant No. 31300484)

REFERENCES CITED

- Chang, L., Chang, X., Chang, H., Qian, W., Cheng, L., and Han, X. (2019). "Nondestructive testing on ancient wooden components based on Shapley value," *Advances in Materials Science and Engineering* 2019, Article ID 8039734. DOI: 10.1155/2019/8039734
- Cheng, J. Q., Yang, J. J., and Liu, P. (1992). *Chinese Wood Journal*, China Forestry Publishing House, Beijing, China.
- Fu, R., Zhang, W., Li, D., and Zhang, H. (2021). "Analyses on chemical composition of ancient wood structural component by using near infrared spectroscopy," *Journal of Forestry Engineering* 6(02), 114-119. DOI: 10.13360/j.issn.2096-1359.202005023
- GB 50005 (2017). "Standard for design of timber structures," Ministry of Housing and Urban-Rural Development of the People's Republic of China, Beijing, China.
- Geng, X. (2018). "Preservation and utilization of historic timber structures," *Study on Natural and Cultural Heritage* 3(06), 76-81. DOI: 10.19490/j.cnki.issn2096-0913.2018.06.013.

- Jiang, Z. H., and Peng, Z. H. (2001). *Wood Properties of the Global Important Tree Species*, Science Press, Beijing, China
- Lu, D. (2017). "Liang Ssu-cheng's "Reintegrate the Aged as Aged" and relevant Western concepts," *Time + Architecture* 2017(06), 2017, 138-143. DOI: 10.13717/j.cnki.ta.2017.06.023
- Mosoarca, M., and Gioncu, V. (2013). "Historical wooden churches from Banat Region, Romania. Damages: Modern consolidation solutions," *Journal of Cultural Heritage* 14(3), 45-59. DOI: 10.1016/j.culher.2012.11.020
- Parisi, M. A., and Piazza, M. (2007). "Restoration and strengthening of timber structures: Principles, criteria, and examples," *Practice Periodical on Structural Design and Construction* 12(4), 177-185. DOI: 10.1061/(ASCE)1084-0680(2007)12:4(177)
- Qiao, G., Li, T., and Chen, Y. F. (2016). "Assessment and retrofitting solutions for an historical wooden pavilion in China," *Construction and Building Materials* 105, 435-447. DOI: 10.1016/j.conbuildmat.2015.12.107
- Qin, S. J., Yang, N., Hu, H. R., and Zhang, L. (2018). "Study on dynamic characteristics of a damaged ancient timber structure of Ming-Qing dynasty," *Journal of Building Structures* 39(10), 130-137. DOI: 10.14006/j.jzjgxb.2018.10.015
- Shan, S. Y. (1988). "A textual research on the three south schools of the Forbidden City," *Palace Museum Journal* (03), 20-22. DOI: 10.16319/j.cnki.0452-7402.1988.03.004
- Spriggs, J. A., Rowell, R. M., and Barbour, R. J. (1989). "Archaeological wood properties, chemistry, and preservation," *Journal of Field Archaeology* 18(2), 249. DOI: 10.2307/530270
- Shi, Z., M., Zhou, Q., Jin, H. K., and Zhang, X. Q. (2009). "Study on mechanical problems and strengthening methods on some components of the Taihe Palace in the palace museum," *Sciences of Conservation and Archaeology* 21(01), 15-21. DOI: 10.16334/j.cnki.cn31-1652/k.2009.01.003
- Shan, J. (2016). "Overview of the 100-year overhaul of the Forbidden City and the 'Safe Forbidden City' project," *Heritage Architecture* 2016(02), 1-11. DOI: 10.19673/j.cnki.ha.2016.02.002
- Wang, Z., Xie, W.B., Lu, Y., Li, H.T., and Wang, Z.H. (2019). "Dynamic and static testing methods for shear modulus of oriented strand board," *Construction and Building Materials*, 216:542-551. DOI: 10.1016/j.conbuildmat.2019.05.004
- Yin, S. C., Song, J. Z., and Wu, D., Q. (1987). "Study of physical and mechanical properties of *Platycarya strobilacea*," *Journal of Nanjing Forestry University* (02), 58-66. DOI: 10.3969/j.jssn.1000-2006.1987.02.008
- Zhang, Y., Zhu, H., Wang, Z., and Dauletbek, A. (2021). "Analysis of the Influence of Accelerometer Quality and Installation Position on the Test Value of Wood Material Constant," *Experimental Techniques*, 1-15. DOI: 10.1007/s40799-021-00512-x
- Zhao, Y., Ren, J., Zheng, X. X., Pan, B., and Leng, W., Q. (2021). "Effects of three kinds of fungi on color, chemical composition and route of infection of *Picea sitchensis*," *J. Forestry Eng.* 6(06), 88-93. DOI: 10.13360 /j.issn.2096-1359.202104007

Article submitted: September 23, 2021; Peer review completed: November 6, 2021;
Revised version received and accepted: December 10, 2021; Published: December 15, 2021.

DOI: 10.15376/biores.17.1.962-974